Grass Research

ARTICLE

Open Access

https://doi.org/10.48130/grares-0025-0009

Grass Research **2025**, 5: e013

Comparative physiological and transcriptomic analyses of zoysiagrass (*Zoysia japonica*) species reveal key metabolic pathways for salt tolerance

Zhenzhen Liu[1], Shu Ma[1], Xinxin Xu[1], Jiayue Sun[2], Mingna Li[3], Yan Sun[1], Kehua Wang[1], Peisheng Mao[1] and Xiqing Ma[1*]

[1] *College of Grassland Science and Technology, China Agricultural University, Beijing 100193, China*
[2] *Qingdao Haiyuan Turfgrass Co., Ltd., Qingdao 266300, Shandong, China*
[3] *Institute of Animal Science, Chinese Academy of Agricultural Sciences, Beijing 100193, China*
* Corresponding author, E-mail: ma2016@cau.edu.cn

Abstract

Soil salinity is a significant environmental challenge that adversely affects plant yield and quality. Zoysiagrass (*Zoysia japonica*), a member of the Gramineae family, is highly salt-tolerant, making it an excellent model for studying salt stress response mechanisms. We performed physiological and transcriptomic analyses on two contrasting Zoysiagrass germplasm accessions under high salt conditions. The salt-tolerant germplasm ST68 demonstrated superior growth phenotypes, higher chlorophyll and relative water content, greater photochemical efficiency, and lower relative electrolyte leakage and sodium ion content compared to the salt-sensitive germplasm SS9. Transcriptomic analysis revealed differential expression in pathways involved in photosynthesis, flavonoid biosynthesis, cell wall macromolecule catabolism, phosphate ion homeostasis, and reactive oxygen species response in the tolerant vs the sensitive line under salt stress. Notably, the *ZjHEMA* gene, which encodes glutamyl-tRNA reductase, a rate-limiting enzyme in chlorophyll biosynthesis, was identified as a key regulator due to its significant upregulation under salt stress in the salt-tolerant germplasm, compared to the sensitive one. Overexpression of the salt-responsive glutamyl-tRNA reductase gene, associated with chlorophyll metabolism in Zoysiagrass, in Arabidopsis led to increased salt tolerance, as evidenced by elevated chlorophyll content, relative water content, and photochemical efficiency compared to wild-type plants. Our findings offer new insights into the mechanisms of salt tolerance in Zoysiagrass, laying a foundation for breeding salt-tolerant germplasm.

Citation: Liu Z, Ma S, Xu X, Sun J, Li M, et al. 2025. Comparative physiological and transcriptomic analyses of zoysiagrass (*Zoysia japonica*) species reveal key metabolic pathways for salt tolerance. *Grass Research* 5: e013 https://doi.org/10.48130/grares-0025-0009

Introduction

Soil salinization, a type of abiotic stress, presents a significant global challenge, particularly in arid and semi-arid regions where it drastically curtails agricultural productivity[1–5]. It is estimated that salt stress and alkalinity impact approximately 1 billion hectares of land worldwide, constituting 7% of the Earth's surface and over 20% of all arable land[6,7]. In China alone, soil salinization affects about 4.88% of usable land and 9.91 million hectares of arable land[8]. High soil salinity impairs plants' ability to absorb water due to osmotic pressure, disrupts physiological processes by accumulating excessive amounts of specific ions like Na^+ and Cl^-, and leads to nutrient imbalances that further reduce plant viability[7,9–11].

Investigating how plants respond to salt stress is crucial for developing effective management strategies and enhancing their overall adaptability[12]. Plants have evolved various morphological, physiological, biochemical, and molecular adaptations to thrive under salt stress[13]. In terms of physiological mechanisms, the plant alleviates salt damage through salt excretion, dilution, accumulation, and avoidance, and enhances salt tolerance through osmotic regulation and active oxygen scavenging[14]. In the osmotic regulation mechanism, plant cells maintain water balance by accumulating organic solutes and inorganic ions. Organic solutes include proline, betaine, soluble sugars, and polyols, among which proline enhances hydration by binding to proteins at the hydrophobic end, effectively preventing protein denaturation under osmotic stress. Betaine plays multiple protective roles by maintaining membrane integrity, stabilizing enzyme activity, and protecting chloroplast function. Inorganic ions (K^+, Na^+, Cl^-) protect plant cells by dynamically regulating their osmotic pressure[15–19]. It has been confirmed that the synergistic effect of solutes significantly improves the stability of plant cells under salt stress[20]. The antioxidant enzyme system in plants evolved through long-term evolutionary processes, constitutes a conserved defense mechanism that synergistically complements physiological adaptations to environmental stressors. It mainly consists of enzymatic antioxidants, such as APX (ascorbate peroxidase), CAT (catalase), POD (peroxidase), SOD (superoxide dismutase), MDHAR (monodehydroascorbate reductase), DHAR (dehydroascorbate reductase), GR (glutathione reductase), GPX (glutathione peroxidase), and GST (glutathione S-transferase), as well as non-enzymatic antioxidants, including AsA (ascorbic acid), GSH (glutathione), CAR (carotenoid), α-tocopherol, and some alkaloids and flavonoids[16]. The activity of antioxidant enzymes in plant chloroplasts-such as SOD, APX, POD, GPX, GST, and CAT is enhanced to counteract oxidative damage from excess reactive oxygen species under salt stress[12]. At the same time, non-enzymatic antioxidants also play a crucial role in plant tolerance to salt stress. AsA often acts as a potent antioxidant, directly scavenging reactive oxygen species (ROS) under stress. It not only regulates cellular oxidation but also participates in the formation of alpha-tocopherol[21]. As an important signaling molecule regulating cellular reduction-oxidation status, AsA plays a key role in processes such as photosynthesis and mitochondrial electron transfer[21]. Signal transduction in plants intersects under stress conditions, forming a complex network that regulates the plant's response to salt stress. Based on the involvement of Ca^{2+} in the signaling process, these pathways can be categorized into two groups: Ca^{2+}-dependent and Ca^{2+}-independent signal transduction pathways (e.g., MAPK pathway)[16]. Ca^{2+}-dependent signal transduction pathways mainly include the salt overly sensitive (SOS), abscisic acid (ABA), and

calcium-dependent protein kinase (CDPK) pathways. In these pathways, Ca^{2+} not only acts as an osmoregulatory molecule but also functions as a signaling molecule in the salt stress response. It primarily regulates its concentration in plant cells through Ca^{2+} channels, triggering a cascade of distinct signaling pathways[22]. As one of the most important signal transduction pathways in plants, the MAPK cascade amplifies environmental signals through protein kinase-catalyzed phosphorylation, thereby transmitting signals from the cell surface to the interior[23].

Gene function mining is a prerequisite for studying the molecular mechanisms of plant responses to salt stress. Currently, functional studies of salt-responsive genes in plants mainly focus on antioxidants, osmotic stress, ion transporters, and signal transduction[16]. It has been found that the salinity tolerance of plants under salt stress is related to their photosynthetic capacity[24]. For most plants, salt stress affects chlorophyll structure and reduces chlorophyll content, leading to a decrease in the photosynthetic rate[25]. This is mainly achieved by directly affecting the activity and expression levels of enzymes involved in chlorophyll biosynthesis and photosynthesis[26]. Under salt stress, the chlorophyll and carotenoid contents of lentil seedlings were significantly reduced. Exogenous application of glutamate effectively reduced the accumulation of Na^+ in lentil seedlings, significantly improving seedling survival rates[27]. Chlorophyll content in plants is significantly correlated with salt tolerance, and its increase can notably improve salt tolerance[28]. The chlorophyll biosynthesis pathway begins with the conversion of glutamate to glutamyl-tRNA, with GluTR serving as a key rate-limiting enzyme in the upstream regulation of 5-aminolevulinic acid (ALA), playing a crucial role in chlorophyll biosynthesis and plant growth[29,30]. The mutation of the *ZmGluTR1* gene in maize directly caused the mutant to exhibit leaf yellowing, along with decreased chlorophyll intermediates and photosynthetic pigments[31]. Currently, GluTR regulation mainly focuses on transcriptional and post-translational mechanisms, with its regulatory processes involving redox regulation, heme, and so on[32–34]. However, the mechanisms by which GluTR-related genes contribute to plant stress responses have not yet been reported.

Transcriptome sequencing has identified a large number of differentially expressed genes (DEGs) involved in salt stress responses across various species, including rice (*Oryza sativa*)[35], maize (*Zea mays*)[36], soybean (*Glycine max*)[37], cotton (*Gossypium hirsutum*)[20], barley (*Hordeum vulgare*)[38], oat (*Avena sativa*)[39], and black wolfberry (*Lycium ruthenicum*)[40]. The integration of RNA-seq technology with studies of plant morphology and physiology provides a comprehensive approach to understanding plant stress responses[41,42].

Turfgrasses serve crucial economic, environmental, ecological, recreational, and aesthetic functions. However, salinity poses a significant challenge, impairing the growth of both cool- and warm-season turfgrass species in affected regions[20]. Salt stress markedly diminishes turfgrass quality, growth, development, and other functional traits by creating a hyperosmotic effect, which reduces the soil's water potential, making it a significant abiotic factor limiting turfgrass productivity[43]. Therefore, understanding the stress tolerance of turfgrass, especially its salt tolerance, has emerged as a critical research focus[13]. *Zoysia*, a member of the Gramineae family, is a widely utilized warm-season turfgrass genus. Given the considerable variation in salt tolerance among *Zoysia* species, this genus serves as an ideal model for studying the mechanisms of salt tolerance[44–46]. Studies on the salt tolerance of Zoysiagrass mainly focus on the correlation between salt tolerance identification, phenotypic traits, physiological responses, the effects of exogenous substances on salt tolerance, and comparative genomic analyses. For example, Qian et al.[46] evaluated and identified the salt tolerance of 29 Zoysiagrass experimental lines and cultivars, explored the correlation between leaf texture and salt tolerance and examined the growth and physiological phenotypes of different Zoysiagrass germplasm under salt stress[47]. Exogenous application of calcium and spermidine significantly improved the salt tolerance of Zoysiagrass, with calcium promoting the expulsion of Na^+ ions through the salt glands[48,49]. Based on comparative genomics, the genomic characteristics of adaptive evolution in *S. dulcis* were studied, revealing that its stress response is linked to genes related to cytochrome P450 and abscisic acid biosynthesis[50]. However, the physiological and molecular mechanisms underlying the response to salt stress in Zoysiagrass germplasm with varying salt tolerance levels remain less studied and require further exploration. To address this gap, our study employed physiological assessments and RNA-Seq analyses to compare salt stress tolerance between two distinct Zoysiagrass species. Through functional analysis of DEGs, we investigated the role of the chlorophyll metabolism pathway in plant responses to salt stress, laying the groundwork for a deeper understanding of the mechanisms underlying plant responses to salt stress.

Materials and methods

Plant materials and growth conditions

Following the evaluation of 99 Zoysiagrass accessions[49], the salt-tolerant germplasm ST68 and the salt-sensitive germplasm SS9 from Qingdao Haiyuan Turfgrass Co., Ltd. (Qingdao, China) were selected to study the mechanisms of salt responsiveness. Zoysiagrass germplasm accessions were cultivated in round plastic planters (25 cm in diameter, 18 cm in height) filled with a 1:1 (v/v) mixture of peat and vermiculite. They were cultured in an artificial climate chamber with 28/25 °C (day/night) temperatures. The plants were watered weekly with half-strength Hoagland nutrient solution and trimmed weekly to maintain a uniform canopy height.

Treatments and experimental design

After 2 months of establishment in the artificial climate chamber, plants were subjected to salt stress by daily irrigation with increasing concentrations of NaCl in half-strength Hoagland nutrient solution, starting with 80 mM NaCl for one day, followed by 160 mM NaCl for another day, and finally 250 mM NaCl to avoid salt shock. SS9 and ST68 were arranged in a randomized complete block design with four replicates, and physiological measurements were taken at 0, 3, 6, 9, and 12 d of salt stress (250 mM) or control treatment.

Physiological analysis

Photochemical efficiency (Fv/Fm) was measured using the method described by Ma et al.[51] with a portable fluorometer (OPTI-SCIENCES OS-30p+, USA) after a 30 min dark adaptation period. Relative electrolyte leakage (REL) of the leaves was assessed by weighing approximately 0.1 g of fresh leaves, which were washed three times with distilled water and cut into 0.5 cm pieces. These were placed into a clean centrifuge tube containing 30 mL of distilled water and shaken at 200 rpm at 28 °C for 24 h. The initial conductivity (Ci) was measured using an electrical conductivity meter (METTLER TOLEDO FiveEasy Plus FE38). The samples were then autoclaved at 121 °C for 30 min and cooled to room temperature to determine the maximum conductivity (Cmax). The REL of leaves was calculated as (Ci/Cmax) × 100%[52]. Chlorophyll content (a + b) was determined following the procedure outlined in a previous study[53]. Briefly, about 0.1 g of fresh leaves was extracted in 10 mL of dimethyl sulfoxide (DMSO) in the dark for 72 h. The chlorophyll content was measured at 663 nm and 645 nm using a

BECKMAN DU2600 spectrophotometer (Puxi Biological Technology Co., Beijing, China). Relative water content (RWC) was determined as described by Ma et al.[54]. The fresh weight (FW), turgid weight (TW), and dry weight (DW) of the leaf samples were measured independently. Approximately 0.1 g of fresh leaves were harvested, immediately weighed, and recorded as the FW. These leaves were then cut into 0.5 cm pieces, immersed in a centrifuge tube filled with distilled water, and placed in darkness at 4 °C for 24 h. After this period, the leaves were removed and weighed to determine the TW. Subsequently, the soaked leaves were dried at 80 °C for 72 h and weighed again to obtain the DW. RWC was calculated as (FW − DW)/(TW − DW) × 100%[55].

Ion content measurements

After exposure to the salt treatment for 9 d, leaf and root Na^+ and K^+ ion content were measured separately according to the methods described by Ma et al.[51]. Fresh leaves and roots (1 g each) were rinsed with distilled water, dried at 80 °C for 72 h, and ground into a fine powder. The powdered samples were incinerated in a crucible preheated to 500 °C for 4 h. After cooling to room temperature, the ash was dissolved in 10 mL of 0.1 N HCl solution. This solution was then diluted to 50 mL with distilled water and thoroughly mixed. Ion analysis was performed using an inductively coupled plasma atomic emission spectrometer (ICP-AES, 715ES, Varian).

RNA sequencing and transcriptomic analysis

On day 9 of treatment, mature leaves from both the salt-stressed and control groups of SS9 and ST68 were harvested and immediately ground into a fine powder under liquid nitrogen. Total RNA was extracted using the TransZol Up Plus RNA Kit, and RNA integrity was verified on 1% agarose gels to select high-quality samples for sequencing. Libraries for RNA sequencing were prepared using the NEB Next Ultra™ RNA Library Prep Kit and sequenced (150-bp paired-end reads) on an Illumina HiSeq 2500 platform (OE Biotech Co., Ltd., Shanghai, China). Raw sequencing data were filtered using Trimmomatic software, and clean reads were aligned to the Zoysia reference genome available at http://zoysia.kazusa.or.jp/.

Functional annotation of unigenes and analysis of differentially expressed genes

The filtered high-quality reads were aligned to the reference genome. HTSeq-count was utilized to calculate the read counts for each gene, reflecting the baseline expression levels. To account for variances in gene length and sequencing depth, FPKM (Fragments Per Kilobase of transcript per Million mapped reads) was applied, standardizing the expression levels across different genes and samples to ensure comparability. Differential gene expression analysis was conducted using DESeq, with genes identified as differentially expressed based on a threshold of |Fold Change| ≥ 1.5 and a p-value < 0.05. The DEGs were subsequently annotated for protein function using comprehensive databases such as the Kyoto Encyclopedia of Genes and Genomes (KEGG), Gene Ontology (GO), SwissProt, and the NCBI non-redundant protein (NR) database[56].

Functional validation of the *ZjHEMA* gene through gene transformation in *Arabidopsis thaliana*

Total RNA was extracted from the leaves of Zoysiagrass using an RNA extraction kit (TransZol Up Plus) and reverse transcription was performed using a cDNA synthesis SuperMix, which served as a template for cloning. Specific primers (F: 5'-atggacgagctctacaaggtc gacATGGCGAGCGCCCCGTCGGC-3' and R: 5'-cggggaaattcgagctcG GTACCTCAGTTTTGAGTCTTCTCGACCTTGGC-3') were used to amplify the coding region of the *ZjHEMA* gene (*Zjn_sc00092.1.g01460*). The amplified product was cloned into the pSuper1300 over-expression vector via *SalI* and *KpnI* restriction sites. This expression vector was constructed through homologous recombination and was introduced into *Agrobacterium tumefaciens* GV3101 by the freeze-thaw method. Transformation of *Arabidopsis thaliana* was carried out using the floral dip method. Seeds from the T0 generation were sterilized and germinated on selective medium (50 μg/mL kanamycin) following Sun et al.[57] to generate transgenic lines. T3 homozygous seeds were harvested, and RNA was extracted and analyzed for gene expression using the $2^{-\Delta\Delta CT}$ method[57]. The transgenic *Arabidopsis* lines (*ZjHEMA-4* and *ZjHEMA-6*) and wild-type (WT) were seeded into 1/2 MS medium and then transferred to small pots after 7 d. One-month-old seedlings were subjected to an incremental NaCl solution treatment-starting with 50 mM, followed by 100 mM for one day each to avoid salt shock, and then maintained at 150 mM for 12 d. Post-treatment, physiological parameters such as Fv/Fm, REL, chlorophyll content, and RWC were measured as per Ma et al.[54].

Statistical analysis

Data analysis was performed using SPSS 22.0, employing a general linear model for variance analysis of measurements including Na^+ ion content in leaves and roots, salt gland counts, and other variables. Significant differences between treatments were determined using Fisher's least significant difference (LSD) test at $p < 0.05$ and $p < 0.01$, as described by Ma et al.[58]. Data visualization was conducted using Origin 2019 and TBtools[59].

Results

Morphological changes of Zoysiagrass germplasm under salt stress

Two contrasting Zoysiagrass lines, the salt-tolerant line ST68 and the salt-sensitive line SS9-were assessed for morphological and physiological changes in response to 250 mM NaCl (Fig. 1a–c). After 9 d, notable alterations in leaf phenotype were observed in SS9 under salt stress (SS9 + NaCl) compared to the untreated SS9 control, including foliar tip burning, wilting, curling, and water loss. In contrast, ST68 exhibited no obvious changes in leaf phenotype under salt stress compared to the untreated control (Fig. 1b). By day 12, SS9 showed stunted growth, pronounced leaf wilting, drying, and eventually plant death under salt treatment, whereas ST68 exhibited only slight leaf dehydration and drooping under the same conditions (Fig. 1c).

Physiological responses of Zoysiagrass germplasm under salt stress: chlorophyll, RWC, photochemical efficiency, REL, and sodium ion content

Physiological performance including chlorophyll content, RWC, REL, photochemical efficiency (Fv/Fm), and leaf and root Na^+ ion content, were recorded on days 0, 3, 6, 9, and 12 following the salt treatment (Fig. 2). The results indicate that the resistant line ST68 exhibited overall better performance under salt stress compared to the salt-sensitive line SS9. For example, chlorophyll (a + b) content in SS9 was 71.74% lower on day 9 and 69.89% lower on day 12 compared to the non-stressed control. In contrast, ST68 showed no significant difference on day 9, but had a 47.55% increase on day 12 compared with its untreated control (Fig. 2a). The RWC of SS9 decreased by 15.65% and 21.58% on days 9 and 12, respectively, under salt stress compared with the non-stress control, while that of ST68 remained similar to the untreated control throughout the experiment (Fig. 2b). The Fv/Fm ratio in SS9 was reduced by 6.42% and 18.52% compared to the control on days 9 and 12, respectively, whereas that of ST68 showed no significant difference between the treated and untreated groups (Fig. 2c). Moreover, salt stress led to an increase in REL in SS9 (1.96-fold on day 9 and 2.43-fold on day 12 compared to untreated controls) than in ST68 (1.35-fold on day 9

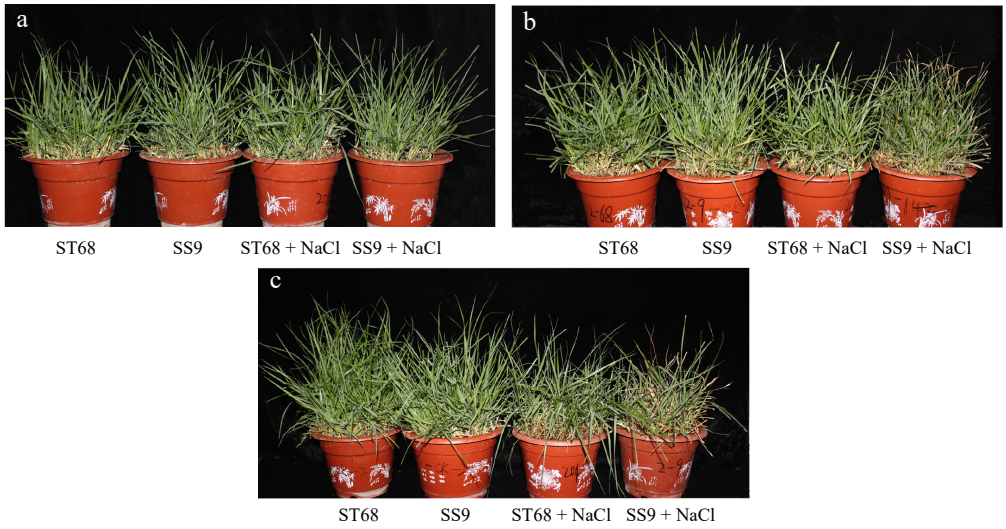

Fig. 1 Phenotypic change of ST68 and SS9 under salt treatment. (a), (b), and (c) show plants treated with 250 mM NaCl for 0, 9, and 12 d, respectively.

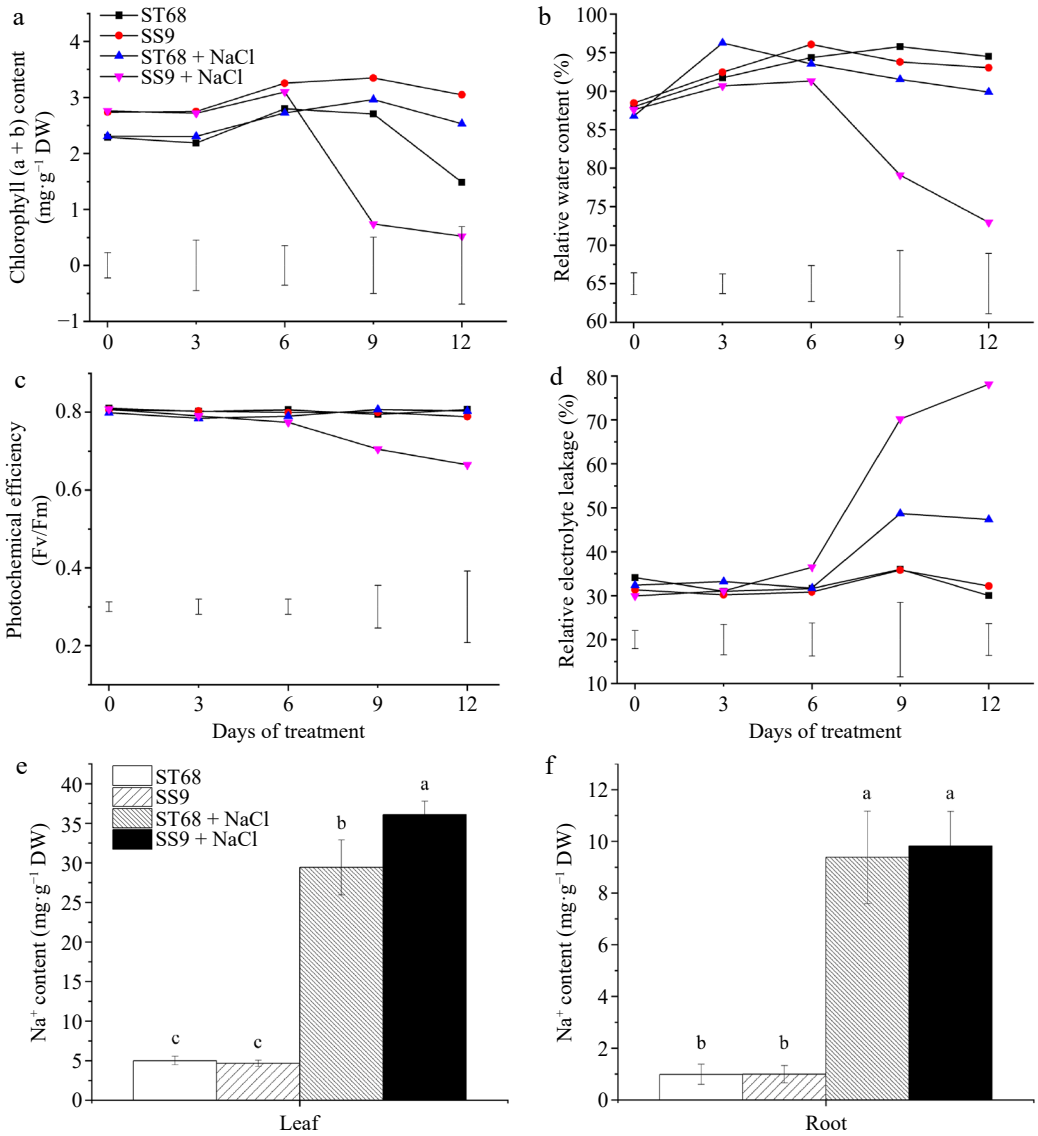

Fig. 2 Physiological performances of ST68 and SS9 under salt stress (250 mM NaCl). (a) Changes in chlorophyll content under salt stress. (b) Changes in relative water content (RWC) under salt stress. (c) Changes in photochemical efficiency (Fv/Fm) under salt stress. (d) Changes in relative electrolyte leakage (REL) under salt stress. (e) Sodium ion content in leaves after 9 d of salt stress. (f) Sodium ion content in roots after 9 d of salt stress. Values of (a)–(d) are means ± LSD and values of (e), (f) are means ± SD, all from four replicates. Different lowercase letters indicate significance at $p < 0.05$.

and ~1.6 fold on day 12 compared to untreated controls) (Fig. 2d). Furthermore, by day 9 of salt treatment, Na^+ ion content significantly increased by 4.89- and 7.73-fold in the leaves of ST68 and SS9 compared with untreated controls; notably, the Na^+ content was significantly higher by 23% in SS9 compared to ST68 under stress, suggesting that fewer Na^+ ions accumulate in the leaves of ST68, thus helping to maintain cellular homeostasis under salt stress (Fig. 2e). Similarly, Na^+ content in the roots of ST68 and SS9 increased by 8.5- and 8.89-fold, respectively, compared with untreated controls, however, no significant differences were observed between the two lines under either treated or untreated conditions (Fig. 2f).

Scanning electron microscope observation of ST68 and SS9 under salt stress

The distribution of salt glands on the leaf surfaces of ST68 and SS9 was examined using scanning electron microscopy (SEM). Salt glands were observed on the leaves of both ST68 and SS9 under salt stress, however, significant differences in gland density were noted (Fig. 3a–c). Specifically, the leaves of ST68 exhibited 1.89-fold more salt glands compared to those of SS9 (Fig. 3a & b). Despite these significant differences in the density of salt glands between the two lines, no significant differences were detected between the salt-stressed plants and their respective control plants within each line (Fig. 3c).

Analysis of DEGs between SS9 and ST68 under salt stress

To elucidate the molecular mechanisms underlying the salt tolerance of the two contrasting Zoysiagrass germplasm accessions, mature blades of ST68 and SS9 under different conditions were collected, mixed, and subjected to transcriptome sequencing. The analysis yielded a total of 96.43 Gb of clean reads with a Q30 percentage of 94.77% and an average GC content of 54.43%. The RNA data from the three biological replicates demonstrated a high correlation in gene expression levels ($R^2 > 0.98$), confirming the reliability of the dataset. These reads were then assembled and used for subsequent analyses (Supplementary Table S1).

As shown in Fig. 4a, a total of 5,243 DEGs were identified in SS9 under salt stress, with 2,275 up-regulated and 2,968 down-regulated, compared to its non-stressed control. Similarly, ST68 exhibited 7,315 DEGs, including 3,854 up-regulated and 3,461 down-regulated genes, under the same conditions. Additionally, under untreated control conditions, 5,647 DEGs (2,727 up-regulated and 2,930 down-regulated) were observed between SS9 and ST68, compared to 10,141 DEGs (4,649 up-regulated and 5,492 down-regulated) between the two lines under salt stress (Fig. 4a). A Venn diagram was utilized to illustrate the similarities and differences in gene expression between the germplasm accessions (Fig. 4b). These findings highlight that the DEGs are germplasm-specific, with ST68 displaying a greater number of DEGs than SS9 when subjected to salt stress.

GO analysis of DEGs

To further investigate differential gene expression between ST68 and SS9 in response to salt stress, DEGs were functionally categorized by GO enrichment analysis. The analyses of DEGs from SS9 + NaCl vs SS9, ST68 + NaCl vs ST68, SS9 vs ST68, and SS9 + NaCl vs ST68 + NaCl comparisons revealed enrichments in 293, 285, 203, and 217 GO terms, respectively (Supplementary Table S2). This analysis reveals germplasm-specific enrichment patterns, highlighting differences in biological processes (BP), cellular components (CC), and molecular functions (MF) between SS9 and ST68 under salt stress conditions. Compared to the susceptible line SS9 (3,330 DEGs), ST68 exhibited a higher number of DEGs (4,366) before and after salt stress, representing a 1.31-fold increase. The most significant GO terms associated with DEGs between the untreated and treated groups of SS9 included nitrate assimilation (GO:0042128), chloroplast (GO:0009507), and nitrate transmembrane transporter activity (GO:0015112) (Supplementary Fig. S1a). In contrast, the top GO assignments for the ST68 vs ST68 + NaCl comparison included chitin (GO:0010200), an integral component of membrane (GO:0016021), and sequence-specific DNA binding (GO:0043565) (Supplementary Fig. S1b).

Response to heat (GO:0009408), chloroplast (GO:0009507), and beta-amylase activity (GO:0016161) were the top pathways up-regulated in both SS9 + NaCl and ST68 + NaCl compared to their

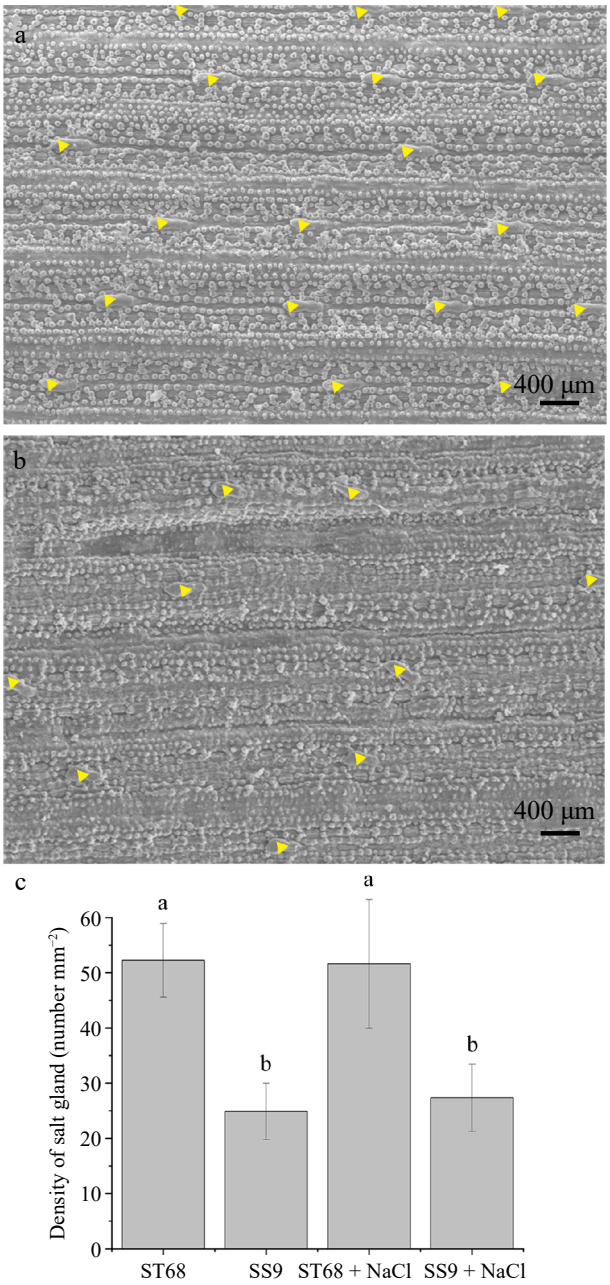

Fig. 3 Distribution and quantification of salt glands in two Zoysiagrass germplasm accessions (ST68 and SS9) under salt stress. (a) Distribution of salt glands on the leaves surface in ST68 + NaCl. (b) Distribution of salt glands on the leaves surface in SS9 + NaCl. (c) Density of salt glands in ST68 and SS9 with and without NaCl treatment. The values are means ± SD from six replicates. Different lowercase letters indicate significance at $p < 0.05$.

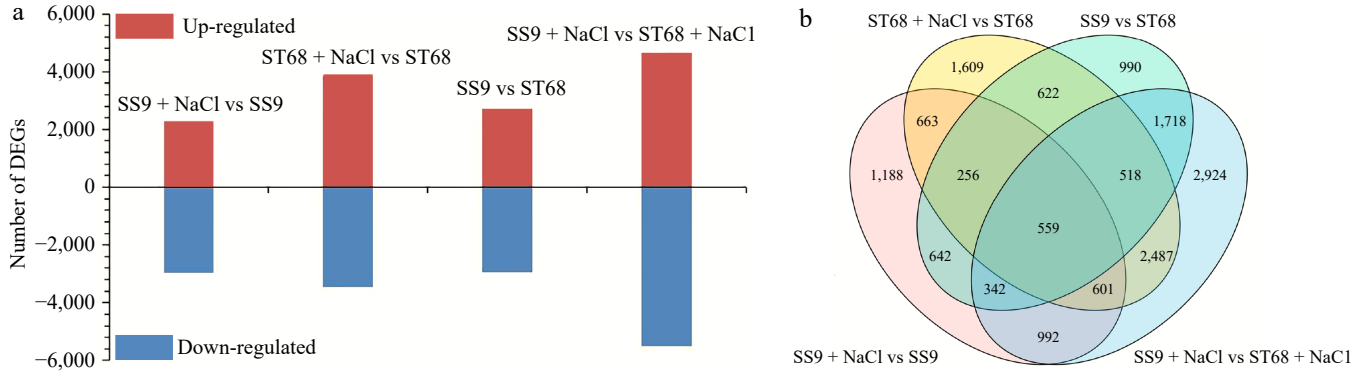

Fig. 4 DEGs identified in ST68 and SS9. (a) Number of DEGs in ST68 and SS9 under unstressed and stressed conditions. (b) Venn diagram illustrating the overlap and unique DEGs between ST68 and SS9 under salt stress.

respective controls (Table 1). Common down-regulated pathways between SS9 + NaCl and ST68 + NaCl compared to their respective controls included chitin response (GO:0010200), an integral component of membrane and protein serine or threonine kinase activity (Table 1). Uniquely up-regulated DEGs in the group SS9 + NaCl vs ST68 + NaCl, compared with the group SS9 vs ST68, were observed in photosynthesis (GO:0015979), chloroplast thylakoid membrane (GO: 0009535), and chlorophyll binding (GO:0016168) (Table 2). Conversely, uniquely down-regulated DEGs under the same conditions included L-phenylalanine, integral component of membrane, and phenylalanine ammonia-lyase activity. This analysis highlights that SS9 and ST68 display unique gene expression profiles and pathway activations under salt stress, revealing key molecular mechanisms that differentiate their responses.

KEGG enrichment analysis of DEGs

To further explore the response mechanisms of the two Zoysia germplasm accessions under salt stress, we analyzed the KEGG enrichment pathways of DEGs between the two germplasm accessions under salt stress and control conditions. The KEGG enrichment analysis revealed that DEGs between the two Zoysiagrass germplasm accessions under salt stress were significantly enriched in pathways associated with photosynthesis, redox homeostasis, and carbohydrate metabolism (Table 3). Notably, the most highly enriched pathway was photosynthesis (ko00195), with 42 DEGs involved, suggesting that salt tolerance may correlate with differential regulation of photosynthetic electron transport and chlorophyll biosynthesis. This is further supported by the enrichment of photosynthesis-antenna proteins (ko00196) and porphyrin and chlorophyll metabolism (ko00860). Additionally, pathways linked to antioxidant defense and osmotic adjustment, such as glutathione metabolism (ko00480), starch and sucrose metabolism (ko00500), amino sugar and nucleotide sugar metabolism (ko00520) were significantly enriched, implying coordinated regulation of ROS scavenging and osmolyte synthesis under salt stress. Intriguingly, nicotinate and nicotinamide metabolism (ko00760) also exhibited strong enrichment, potentially reflecting energy metabolism adaptation to salinity.

DEGs between SS9 and ST68 are enriched for chlorophyll metabolism-related genes under salt stress

The notable upregulation of the chlorophyll metabolism pathway under salt stress prompted further investigation. Differential expression analysis revealed that the SS9 + NaCl vs SS9 comparison exhibited a greater number of DEGs associated with chlorophyll

Table 1. GO terms enriched for DEGs common to SS9 and ST68 in response to salt stress.

Category	Term			ST68 + NaCl vs ST68			SS9 + NaCl vs SS9		
	Name	ID	Pop hits	*p*-adjust	List hits	List total	*p*-adjust	List hits	List total
Commonly up-regulated DEGs									
BP	Response to heat	GO:0009408	177	1.66E-07	40	2374	2.34E-03	19	1,352
CC	Chloroplast	GO:0009507	1,999	5.92E-09	273		4.02E-51	283	
MF	Beta-amylase activity	GO:0016161	18	1.40E-07	10		1.62E-02	3	
Commonly down-regulated DEGs									
BP	Response to chitin	GO:0010200	170	1.08E-18	55	1,992	2.25E-05	33	1,978
CC	Integral component of membrane	GO:0016021	4,892	1.49E-13	542		5.15E-22	579	
MF	Serine/threonine kinase activity	GO:0004674	611	7.06E-07	90		1.65E-03	76	

Table 2. GO terms enriched for DEGs unique to each Zoysiagrass line in response to salt stress.

Category	GO term	ID	Pop hits	Adjusted *p*-value	List hits	List total
Uniquely up-regulated DEGs						
BP	Photosynthesis	GO:0015979	112	1.44E-15	45	2,568
CC	Chloroplast thylakoid	GO:0009535	400	2.06E-12	93	
MF	Chlorophyll binding	GO:0016168	35	3.79E-07	16	
Uniquely down-regulated DEGs						
BP	L-phenylalanine catabolic process	GO:0006559	24	3.50E-08	15	3,143
CC	Integral component of membrane	GO:0016021	4,892	1.31E-08	769	
MF	Phenylalanine ammonia-lyase activity	GO:0045548	18	3.95E-06	11	

Table 3. KEGG enrichment analysis for DEGs of two Zoysiagrass germplasm accessions under salt stress.

Pathway ID	Pathway term	Associated genes number	Enrichment score	Adjusted *p*-value
ko00195	Photosynthesis	42	2.490597262	8.70494E-10
ko00760	Nicotinate and nicotinamide metabolism	16	2.424708445	0.000766994
ko00680	Methane metabolism	39	1.67974868	0.002913442
ko00860	Porphyrin and chlorophyll metabolism	30	1.753583786	0.00503669
ko00196	Photosynthesis-antenna proteins	15	2.116394225	0.00671243
ko00520	Amino sugar and nucleotide sugar metabolism	76	1.394479184	0.00671243
ko00500	Starch and sucrose metabolism	109	1.307902668	0.008129324
ko00480	Glutathione metabolism	53	1.417384716	0.021540316
ko00471	D-Glutamine and D-glutamate metabolism	3	3.068771626	0.046258729
ko00514	Other types of O-glycan biosynthesis	4	2.727797001	0.048753999
ko00902	Monoterpenoid biosynthesis	9	2.045847751	0.048753999

metabolism compared to ST68 + NaCl vs ST68 (Fig. 5). Specifically, a total of 20 chlorophyll metabolism-related DEGs (18 up-regulated and two down-regulated genes) were identified in SS9 + NaCl, and seven such DEGs (four up-regulated and three down-regulated genes) in ST68 were enriched under salt stress conditions compared to their respective controls. Additionally, 14 chlorophyll metabolism-related DEGs (seven up-regulated and seven down-regulated genes) under normal conditions and 23 chlorophyll metabolism-related DEGs (19 up-regulated and four down-regulated genes) under salt-stress conditions were identified in SS9 compared to ST68 (Fig. 5).

Under salt stress conditions, genes encoding glutamyl-tRNA reductase, magnesium chelatase, and protochlorophyllide oxidoreductase exhibited significant differential expression in SS9 and ST68 compared to their respective controls. Comparative analysis between SS9 and ST68 under the salt stress condition revealed that genes encoding key enzymes in chlorophyll metabolism, such as glutamyl-tRNA synthetase, glutamate-1-semiadehyde 2,1-aminomutase, uroporphyrinogen III synthase, uroporphyrinogen III decarboxylase, coproporphyrinogen III oxidase, chlorophyll synthase, and chlorophyll b reductase were specifically expressed in SS9 compared to ST68 under salt stress conditions. Among these DEGs, the expression levels of *ZjHEMD*, *ZjHEMF*, *ZjCHLM*, *ZjPOR,* and *ZjCLH* in SS9 were more than 2-fold higher than in ST68, suggesting these genes may play a crucial role in enhancing salt tolerance. Notably, two genes encoding glutamyl-tRNA-reductase (*ZjHEMA*) and involved in chlorophyll metabolism were differentially expressed between the two lines under salt stress. Specifically, upon salt treatment, the expression level of *Zjn_sc00086.1.g00930* remained unchanged in ST68 but increased by 1.55-fold in SS9, whereas that of *Zjn_sc00092.1.g01460* decreased in both lines, with a greater reduction of 4.11-fold observed in SS9 compared to ST68. These findings reveal that SS9 demonstrates a heightened activation of chlorophyll metabolism-related genes than ST68 under salt stress.

Overexpression of *ZjHEMA* enhances salt tolerance in transgenic *Arabidopsis*

Glutamyl-tRNA reductase is a key rate-limiting enzyme in the synthesis of tetrapyrrole during chlorophyll biosynthesis, and its gene expression differs between ST68 and SS9 under salt treatment. We verified the function of one *ZjHEMA* gene (*Zjn_sc00092.1.g01460*) in regulating salt stress responses through gene transformation in Arabidopsis. Seven independent *Arabidopsis* transgenic lines were obtained, and two lines that showed the highest *ZjHEMA* expression levels were selected for subsequent analyses (Fig. 6a). Growth and morphological and physiological parameters of *ZjHEMA* over-expression (OE) lines were assessed 12 d after treatment with 150 mM NaCl (Fig. 6b).

Under salt stress, the decrease in chlorophyll (a + b) content was significantly lower in the *ZjHEMA* OE lines compared to WT. Specifically, chlorophyll content in *ZjHEMA-4* and *ZjHEMA-6* decreased by only 16.73% and 16.67%, respectively, in contrast to a substantial 54.75% reduction in WT, with *ZjHEMA-4* and *ZjHEMA-6* maintaining 2.08-fold and 1.93-fold higher chlorophyll content than WT, respectively (Fig. 6c). Similarly, the reduction in leaf RWC under salt stress was much less pronounced in the OE lines than in WT-the RWC decreased by only 5.84% and 5.89% in *ZjHEMA-4* and *ZjHEMA-6*, respectively, compared to a 17.55% decrease in WT. As a result, RWC in the OE lines was 7.37% higher than in WT, suggesting improved water retention capability of the OE lines under salt stress (Fig. 6d). While the WT exhibited a significant 21.88% reduction in Fv/Fm under salt stress, the OE lines showed no discernible difference between salt stress and control conditions, and the Fv/Fm ratios of *ZjHEMA-4* and *ZjHEMA-6* were 1.29-fold higher than the WT under stress conditions (Fig. 6e). Moreover, increased REL was observed for all lines under salt stress compared to control conditions; however, the increased in REL was much less prominent for the OE lines than WT. Specifically, the REL of *ZjHEMA-4* and *ZjHEMA-6* was 52.02% and 45.30% lower than that of the WT (Fig. 6f), suggesting better membrane stability and cellular integrity under salt stress conditions. These results confirm that overexpression of *ZjHEMA* significantly enhances salt stress tolerance in Arabidopsis, supporting its critical role in salt tolerance.

Discussion

Salt stress represents a significant environmental constraint that can disrupt osmotic potential and ion levels in plants, ultimately inhibiting cellular metabolism[60]. In high-salt environments, plants have evolved various mechanisms to combat salt stress. These include compartmentalizing ions into salt bladders, secreting excess Na^+ ions through salt glands, or blocking ion transport to aboveground parts via the rhizome junction, thereby reducing Na^+ ion toxicity[61,62]. This study demonstrated that the salt-tolerant Zoysiagrass variety ST68 exhibited superior growth phenotypes, higher chlorophyll content, increased RWC, enhanced photochemical efficiency, reduced REL, and lower Na^+ ion content compared to the salt-sensitive Zoysiagrass germplasm SS9. Further gene expression analysis revealed that overexpression of a gene associated with salt response and photosynthesis in Arabidopsis resulted in enhanced salt tolerance.

Our results indicate that the salt-tolerant Zoysiagrass line ST68 has a higher density of salt glands and lower levels of Na^+ ions in the leaves compared to the salt-sensitive line SS9. This finding aligns with a previous report that salt resistance in Zoysiagrass is positively correlated with the density of salt glands and the rate of salt secretion[63]. The lower Na^+ content and higher density of salt glands may suggest that the tolerant Zoysiagrass line ST68 effectively secretes excess Na^+ ions from the cells through salt glands, thereby maintaining stability in intracellular ion concentrations. Conversely, with fewer salt glands, the salt-sensitive line SS9 accumulates excess Na^+ ions, leading to symptoms such as leaf tip

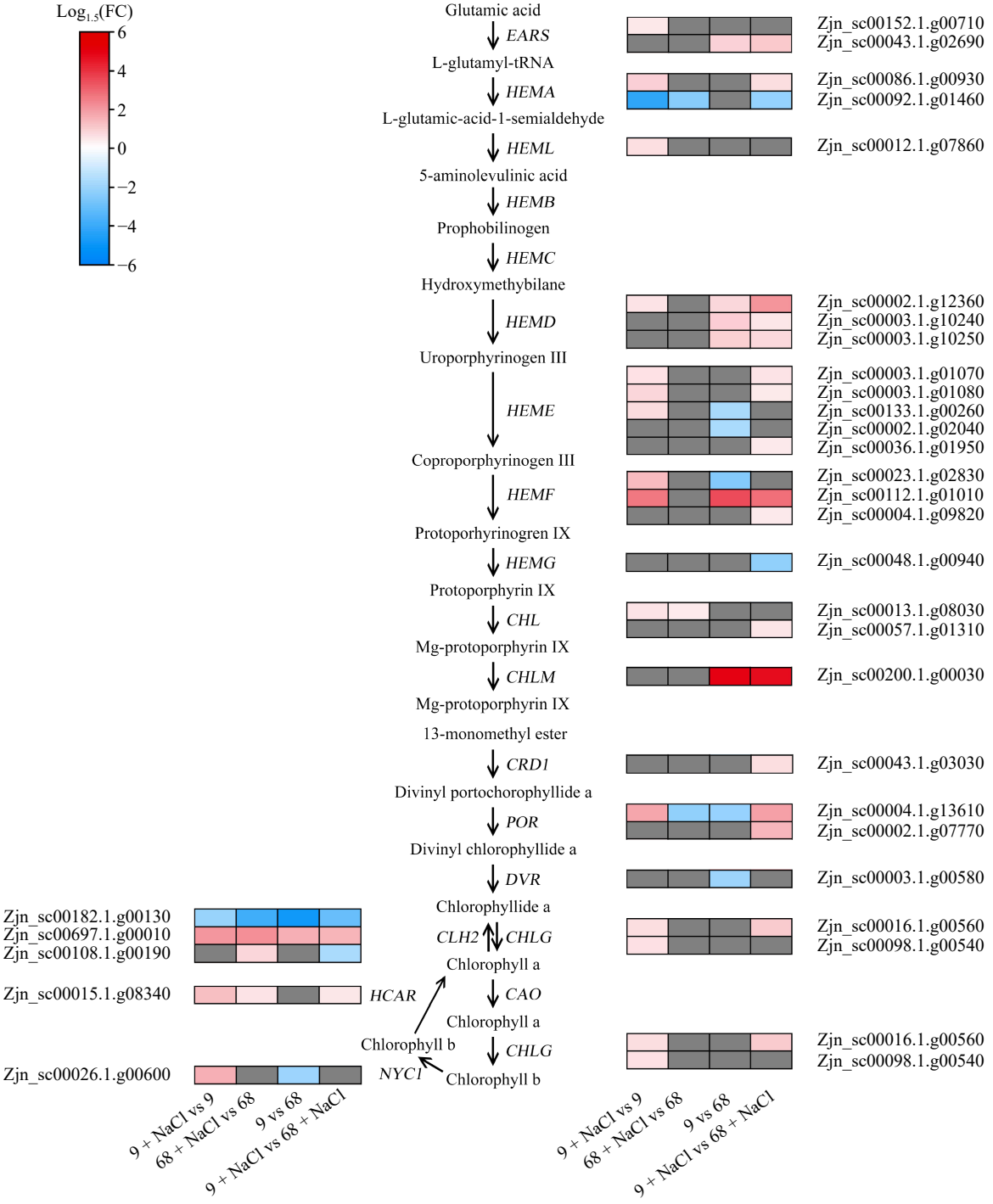

Fig. 5 Expression profiles of DEGs related to chlorophyll metabolism. EARS, glutamyl-tRNA synthetase; HEMA, glutamyl-tRNA reductase; HEML, glutamate-1-semialdehyde 2,1-aminomutase; HEMB, porphobilinogen synthase; HEMC, hydroxymethylbilane synthase; HEMD, uroporphyrinogen III synthase; HEME, uroporphyrinogen III decarboxylase, HEMF, coproporphyrinogen III oxidase; HEMG, protoporphyrinogen oxidase; CHLD, magnesium chelatase; CHLM, magnesium proto IX methyltransferase; CRD1, Mg-protoporphyrin IX monomethyl ester cyclase; POR, protochlorophyllide oxidoreductase; DVR, 3,8-divinyl protochlorophylide a 8-vinyl reductase; CAO, chlorophyllide a oxygenase; CHLG, chlorophyll synthase; NYC1, chlorophyll b reductase; HCAR, 7-hydroxymethyl chlorophyll a reductase.

burning, curling with water loss, and wilting. This mechanism is supported by similar findings in Rhodes grass, where the leaf blades secrete large amounts of salt crystals under salt stress, effectively alleviating salt-induced leaf senescence and physiological damage[64,65].

The observation that ST68 exhibited greater RWC, Fv/Fm, and chlorophyll (a + b) content compared to SS9 aligns with findings in salt-tolerant *Bromus inermis* under similar conditions[66]. Transcriptome analysis revealed enrichment of DEGs in pathways related to chloroplasts, beta-amylase activity, serine/threonine kinase activity, and response to chitin in both salt-sensitive and salt-tolerant plants under salt stress conditions. Among these, genes involved in the serine/threonine kinase activity metabolic pathway are significantly associated with plant salt tolerance[67]. However, the two Zoysia germplasm accessions displayed distinct response mechanisms, with ST68 showing upregulation of genes related to

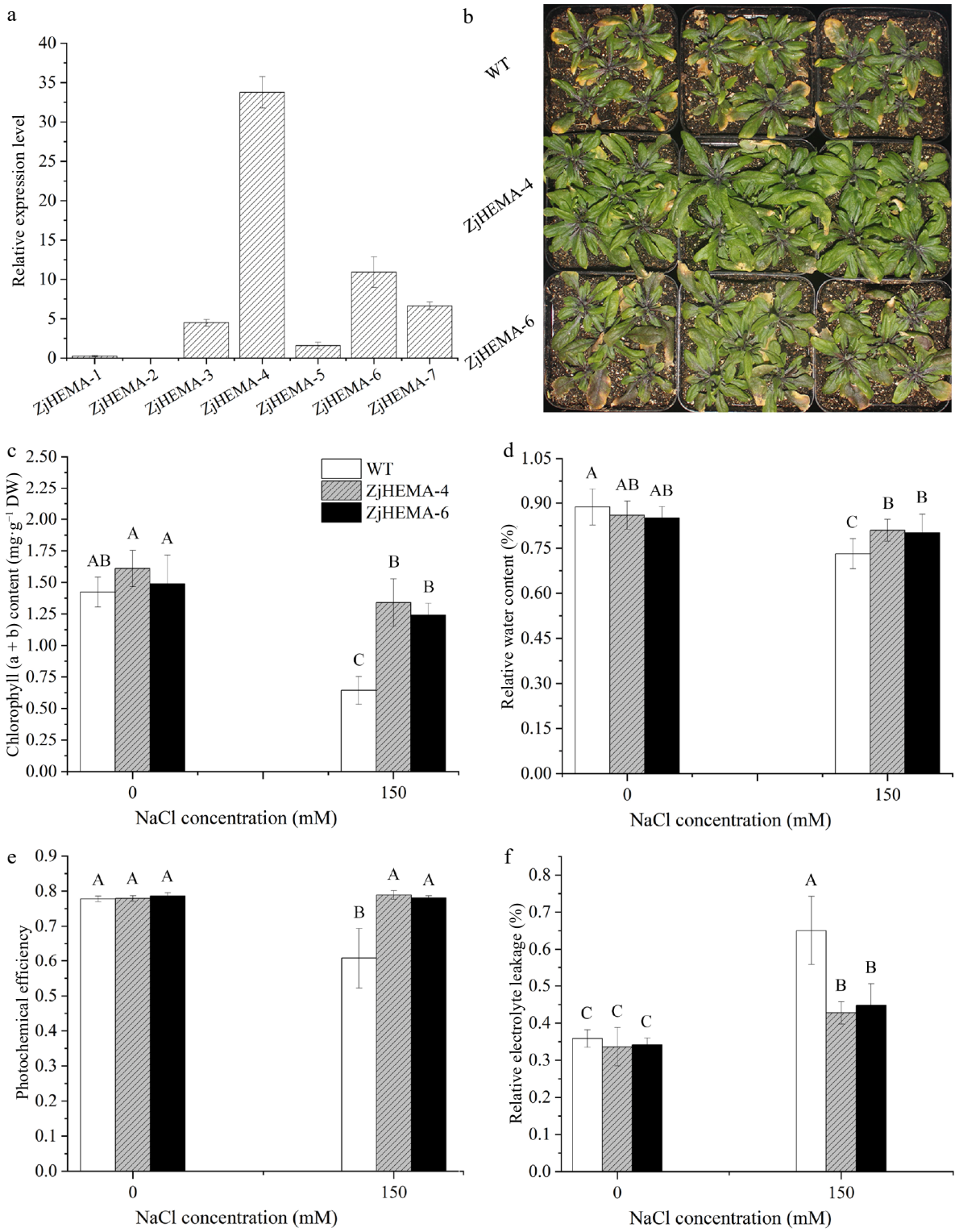

Fig. 6 Morphological and physiological responses of *ZjHEMA* overexpression *Arabidopsis* lines under salt stress. (a) Relative expression levels of *ZjHEMA* in *Arabidopsis* transgenic lines. *AtUBQ* served as the endogenous control. (b) Plant morphologies of the WT and *ZjHEMA* OE lines under salt stress. (c) Chlorophyll (a + b) contents in the WT and *ZjHEMA* OE lines. (d) RWC of the WT and *ZjHEMA* OE lines. (e) Fv/Fm ratios of WT and *ZjHEMA* OE lines. (f) REL of the WT and *ZjHEMA* OE lines. The values are means ± SD from four replicates. Different uppercase letters indicate significance at $p < 0.01$.

photosynthesis, chloroplast thylakoids, and chlorophyll binding. This adaptation likely facilitates enhanced CO_2 concentration and chloroplast function under salt stress, critical for maintaining photosynthesis and mitigating oxidative stress by eliminating excessive reactive oxygen species generated under such conditions[68–70]. Based on the transcriptome sequencing of ST68 and SS9 under salt stress, we discovered that DEGs in salt-tolerant germplasm ST68 and salt-sensitive germplasm SS9 were enriched in three photosynthetic pathways, such as photosynthesis (ko00195), porphyrin and chlorophyll metabolism (ko00860), and photosystem-antenna proteins (ko00196). This finding is consistent with research by Ryu & Cho, which suggests that salt tolerance in plants increases with enhanced

photosynthesis[24]. Zhao et al. found that overexpression of the light-harvesting chlorophyll a/b-binding protein MdLhcb4.3 in apple significantly enhanced the tolerance of transgenic apple callus and transgenic *Arabidopsis* to osmotic stress[71]. Additionally, DEGs in salt-tolerant germplasm ST68 and salt-sensitive germplasm SS9 were significantly enriched in the glutathione metabolic pathway (ko00480), where NADPH-dependent glutathione reductase catalyzes the reduction of glutathione, removes excessive ROS generated under salt stress, and enhances plant salt tolerance[72].

Notably, we validated a key gene in the chlorophyll metabolic pathway that was differentially expressed between SS9 and ST68 under salt stress conditions. Sequence analysis identified this gene as *ZjHEMA1*, one of three *HEMA* genes encoding glutamyl-tRNA reductase, a rate-limiting enzyme essential for the synthesis of tetrapyrrole compounds, such as chlorophyll, predominantly expressed in the green parts of plants. Previous studies have revealed that GluTR exists in multiple copies in higher plants, and it is encoded by three *HEMA* genes (*HEMA1*, *HEMA2*, *HEMA3*) in *Arabidopsis thaliana*, with the GluTR1 and GluTR2 subtypes being predominant. Among them, GluTR1 is encoded by *HEMA1* and is primarily expressed in the green parts of plants[31,33]. Overexpression of *ZjHEMA1* in Arabidopsis resulted in enhanced salt tolerance compared to the WT, mirroring the effects seen in *OsHEMA1* overexpression lines in rice under salt stress[68]. The salt tolerance associated with *ZjHEMA1* seen here is supported by the role of glutamyl-tRNA reductase in ALA production. Glutamyl-tRNA reductase catalyzes the conversion of L-glutamyl-tRNA to L-glutamic acid-1-semialdehyde (GSA), releasing tRNA-a key regulatory step in chlorophyll synthesis[73]. The unstable intermediate GSA is subsequently isomerized to ALA by GSA aminotransferase[68,74]. ALA serves as the precursor for all tetrapyrroles and protochlorophyllide, which converts to chlorophyll upon exposure to light[75]. ALA is also known to enhance plant stress tolerance[76,77]. However, the specific mechanisms by which ALA enhances salt tolerance in plants warrant further investigation.

Conclusions

Soil salinization is a serious global problem that can severely limit agricultural production. In this study, we analyzed two contrasting Zoysiagrass germplasm accessions, the salt-tolerant ST68, and the salt-sensitive SS9, under high salt conditions. ST68 exhibited superior growth, higher chlorophyll, and water content, and enhanced photochemical efficiency. Additionally, transcriptomic analysis revealed differential expression in key pathways such as photosynthesis and flavonoid biosynthesis. Moreover, we validated the role of one DEG between ST68 and SS9, a salt-responsive glutamyl-tRNA reductase gene involved in chlorophyll metabolism, in conferring salt tolerance through *Arabidopsis* transformation experiments. The findings of this research provide valuable insights into the physiological and molecular mechanisms underlying salt tolerance in Zoysiagrass and a candidate gene for improving salt resistance in Zoysiagrass and related species through breeding or genetic engineering.

Author contributions

The authors confirm their contribution to the paper as follows: study conception and design: Ma X; data collection: Liu Z, Ma S, Xu X, Sun J; analysis and interpretation of results: Liu Z, Ma X, Sun Y; draft manuscript preparation: Liu Z, Li M, Mao P, Wang K, Ma X. All authors reviewed the results and approved the final version of the manuscript.

Data availability

The relevant data have been uploaded to the NCBI Sequence Read Archive database. The related link is www.ncbi.nlm.nih.gov/sra, with Submission ID SUB6925943 and BioProject ID PRJNA604914.

Acknowledgments

This research was supported by National Key Research and Development Program of China (2023YFD1200300), and the earmarked fund for CARS (CARS-34).

Conflict of interest

The authors declare that they have no conflict of interest.

Supplementary information accompanies this paper at (https://www.maxapress.com/article/doi/10.48130/grares-0025-0009)

Dates

Received 30 December 2024; Revised 18 February 2025; Accepted 20 February 2025; Published online 9 April 2025

References

1. Meng X, Liu S, Dong T, Xu T, Ma D, et al. 2020. Comparative transcriptome and proteome analysis of salt-tolerant and salt-sensitive sweet potato and overexpression of *IbNAC7* confers salt tolerance in *Arabidopsis*. *Frontiers in Plant Science* 11:572540
2. Abid M, Gu S, Zhang Y, Sun S, Li Z, et al. 2022. Comparative transcriptome and metabolome analysis reveal key regulatory defense networks and genes involved in enhanced salt tolerance of *Actinidia* (kiwifruit). *Horticulture Research* 9:uhac189
3. Mohamed IAA, Shalby N, El-Badri AM, Batool M, Wang C, et al. 2022. RNA-seq analysis revealed key genes associated with salt tolerance in rapeseed germination through carbohydrate metabolism, hormone, and MAPK signaling pathways. *Industrial Crops and Products* 176:114262
4. Negrão S, Courtois B, Ahmadi N, Abreu I, Saibo N, et al. 2011. Recent updates on salinity stress in rice: from physiological to molecular responses. *Critical Reviews in Plant Sciences* 30:329–77
5. Zhang J, Flowers TJ, Wang S. 2010. Mechanisms of sodium uptake by roots of higher plants. *Plant and Soil* 326:45–60
6. Morton MJL, Awlia M, Al-Tamimi N, Saade S, Pailles Y, et al. 2019. Salt stress under the scalpel – dissecting the genetics of salt tolerance. *The Plant Journal* 97:148–63
7. Hopmans JW, Qureshi AS, Kisekka I, Munns R, Grattan SR, et al. 2021. Critical knowledge gaps and research priorities in global soil salinity. *Advances in Agronomy* 169:1–191
8. Dagar JC, Gupta SR. 2020. Agroforestry interventions for rehabilitating salt-affected and waterlogged marginal landscapes. In *Agroforestry for Degraded Landscapes*, eds. Dagar JC, Gupta SR, Teketay D. Singapore: Springer. pp. 111–62. doi: 10.1007/978-981-15-6807-7_5
9. Läuchli A, Grattan SR. 2011. Plant responses to saline and sodic conditions. In *Agricultural Salinity Assessment and Management*, eds Wallendar WW, Tanji KK. Reston, VA: American Society of Civil Engineers (ASCE). pp. 169–205. doi: 10.1061/9780784411698.ch06
10. Xu Z, Wang M, Ren T, Li K, Li Y, et al. 2021. Comparative transcriptome analysis reveals the molecular mechanism of salt tolerance in *Apocynum venetum*. *Plant Physiology and Biochemistry* 167:816–30
11. Van Zelm E, Zhang Y, Testerink C. 2020. Salt tolerance mechanisms of plants. *Annual Review of Plant Biology* 71:403–33
12. Zhu D, Liu J, Duan W, Sun H, Zhang L, et al. 2023. Analysis of the chloroplast crotonylome of wheat seedling leaves reveals the roles of crotonylated proteins involved in salt-stress responses. *Journal of Experimental Botany* 74:2067–82

13. Jiang Y. 2023. Application of gamma-aminobutyric acid and nitric oxide on turfgrass stress resistance: current knowledge and perspectives. *Grass Research* 3:3
14. Hao S, Wang Y, Yan Y, Liu Y, Wang J, et al. 2021. A review on plant responses to salt stress and their mechanisms of salt resistance. *Horticulturae* 7:132
15. Liang X, Zhang L, Natarajan SK, Becker DF. 2013. Proline mechanisms of stress survival. *Antioxidants & Redox Signaling* 19:998–1011
16. Jiang J, Guo Z, Sun X, Jiang Y, Xie F, et al. 2023. Role of proline in regulating turfgrass tolerance to abiotic stress. *Grass Research* 3:2
17. Uddin MK, Juraimi AS. 2013. Salinity tolerance turfgrass: history and prospects. *The Scientific World Journal* 2013:409413
18. Byerrum RU, Sato CS, Ball CD. 1956. Utilization of betaine as a methyl group donor in tobacco. *Plant Physiology* 31:374–77
19. Guo J, Lu X, Tao Y, Guo H, Min W. 2022. Comparative ionomics and metabolic responses and adaptive strategies of cotton to salt and alkali stress. *Frontiers in Plant Science* 13:871387
20. Hasanuzzaman M, Bhuyan MHM, Anee TI, Parvin K, Nahar K, et al. 2019. Regulation of ascorbate-glutathione pathway in mitigating oxidative damage in plants under abiotic stress. *Antioxidants* 8:384
21. Singh N, Bhardwaj RD. 2016. Ascorbic acid alleviates water deficit induced growth inhibition in wheat seedlings by modulating levels of endogenous antioxidants. *Biologia* 71:401–13
22. White PJ, Broadley MR. 2003. Calcium in plants. *Annals of Botany* 92:487–511
23. Colcombet J, Hirt H. 2008. *Arabidopsis* MAPKs: a complex signalling network involved in multiple biological processes. *The Biochemical Journal* 413:217–26
24. Ryu H, Cho YG. 2015. Plant hormones in salt stress tolerance. *Journal of Plant Biology* 58:147–55
25. Sudhir P, Murthy SDS. 2004. Effects of salt stress on basic processes of photosynthesis. *Photosynthetica* 42:481–86
26. Yang Z, Li JL, Liu LN, Xie Q, Sui N. 2020. Photosynthetic regulation under salt stress and salt-tolerance mechanism of sweet *Sorghum*. *Frontiers in Plant Science* 10:1722
27. Fardus J, Hossain MS, Fujita M. 2021. Modulation of the antioxidant defense system by exogenous L-glutamic acid application enhances salt tolerance in lentil (*Lens culinaris* Medik.). *Biomolecules* 11:587
28. Zhang X, Goatley M, Wang K, Conner J, Brown I, et al. 2023. Methyl jasmonate enhances salt stress tolerance associated with antioxidant and cytokinin alteration in perennial ryegrass. *Grass Research* 3:6
29. Xu L, Zhang W, Niu D, Liu X. 2024. Effects of abiotic stress on chlorophyll metabolism. *Plant Science* 342:112030
30. Jahn D, Verkamp E, Söll D. 1992. Glutamyl-transfer RNA: a precursor of heme and chlorophyll biosynthesis. *Trends in Biochemical Sciences* 17:215–18
31. Yang W, Yuan Y, Yang P, Li S, Ma S, et al. 2023. *ZmGluTR1* is involved in chlorophyll biosynthesis and is essential for maize development. *Journal of Plant Physiology* 290:154115
32. Hou Z, Yang Y, Hedtke B, Grimm B. 2019. Fluorescence in blue light (FLU) is involved in inactivation and localization of glutamyl-tRNA reductase during light exposure. *The Plant Journal* 97:517–29
33. Richter AS, Banse C, Grimm B. 2019. The GluTR-binding protein is the heme-binding factor for feedback control of glutamyl-tRNA reductase. *Elife* 13:e46300
34. Wang P, Liang F, Wittmann D, Siegel A, Shan S, et al. 2018. Chloroplast SRP43 acts as a chaperone for glutamyl-tRNA reductase, the rate-limiting enzyme in tetrapyrrole biosynthesis. *Proceedings of the National Academy of Sciences of the United States of America* 115:E3588–E3596
35. Xie Z, Wang J, Wang W, Wang Y, Xu J, et al. 2021. Integrated analysis of the transcriptome and metabolome revealed the molecular mechanisms underlying the enhanced salt tolerance of rice due to the application of exogenous melatonin. *Frontiers in Plant Science* 11:618680
36. Zhang X, Liu J, Huang Y, Wu H, Hu X, et al. 2022. Comparative transcriptomics reveals the molecular mechanism of the parental lines of maize hybrid An'nong876 in response to salt stress. *International Journal of Molecular Sciences* 23:5231
37. Zeng A, Chen P, Korth KL, Ping J, Thomas J, et al. 2019. RNA sequencing analysis of salt tolerance in soybean (*Glycine max*). *Genomics* 111:629–35
38. Sallam A, Alqudah AM, Dawood MFA, Baenziger PS, A Börner. 2019. Drought stress tolerance in wheat and barley: advances in physiology, breeding and genetics research. *International Journal of Molecular Sciences* 20:3137
39. Xu Z, Chen X, Lu X, Zhao B, Yang Y, et al. 2021. Integrative analysis of transcriptome and metabolome reveal mechanism of tolerance to salt stress in oat (*Avena sativa* L.). *Plant Physiology and Biochemistry* 160:315–28
40. Wang Z, Zhang W, Huang W, Biao A, Lin S, et al. 2023. Salt stress affects the fruit quality of *Lycium ruthenicum* Murr. *Industrial Crops and Products* 193:116240
41. Kou S, Chen L, Tu W, Scossa F, Wang Y, et al. 2018. The arginine decarboxylase gene *ADC1*, associated to the putrescine pathway, plays an important role in potato cold-acclimated freezing tolerance as revealed by transcriptome and metabolome analyses. *The Plant Journal* 96:1283–98
42. Qin X, Yin Y, Zhao J, An W, Fan Y, et al. 2022. Metabolomic and transcriptomic analysis of *Lycium chinese* and *L. ruthenicum* under salinity stress. *BMC Plant Biology* 22:8
43. Ahn JH, Kim JS, Kim S, Soh HY, Shin H, et al. 2015. *De novo* transcriptome analysis to identify anthocyanin biosynthesis genes responsible for tissue-specific pigmentation in Zoysiagrass (*Zoysia japonica* Steud.). *PLoS ONE* 10:e0137943
44. Zhang J, Zhang Z, Liu W, Li L, Han L, et al. 2022. Transcriptome analysis revealed a positive role of ethephon on chlorophyll metabolism of *Zoysia japonica* under cold stress. *Plants* 11:442
45. Marcum KB, Anderson SJ, Engelke MC. 1998. Salt gland ion secretion: a salinity tolerance mechanism among five zoysiagrass species. *Crop Science* 38:806–10
46. Qian Y, Engelke MC, Foster MJV. 2000. Salinity effects on zoysiagrass cultivars and experimental lines. *Crop Science* 40:488–92
47. Hooks T, Masabni J, Ganjegunte G, Sun L, Chandra A, et al. 2022. Salt tolerance of seven genotypes of zoysiagrass (*Zoysia* spp.). *Technology in Horticulture* 2:8
48. Maeda Y. 2019. Effects of calcium application on the salt tolerance and sodium excretion from salt glands in zoysiagrass (*Zoysia japonica*). *Grassland Science* 65:189–96
49. Li S, Jin H, Zhang Q. 2016. The effect of exogenous spermidine concentration on polyamine metabolism and salt tolerance in zoysiagrass (*Zoysia japonica* Steud) subjected to short-term salinity stress. *Frontiers in Plant Science* 7:1221
50. Wang W, Shao A, Xu X, Fan S, Fu J. 2022. Comparative genomics reveals the molecular mechanism of salt adaptation for zoysiagrasses. *BMC Plant Biology* 22:355
51. Ma X, Zhang J, Huang B. 2016. Cytokinin-mitigation of salt-induced leaf senescence in perennial ryegrass involving the activation of antioxidant systems and ionic balance. *Environmental and Experimental Botany* 125:1–11
52. Blum A, Ebercon A. 1981. Cell membrane stability as a measure of drought and heat tolerance in wheat. *Crop Science* 21:43–47
53. Arnon DI. 1949. Copper enzymes in isolated chloroplasts. Polyphenoloxidase in *Beta vulgaris*. *Plant Physiology* 24:1–15
54. Ma X, Zhang J, Burgess P, Rossi S, Huang B. 2018. Interactive effects of melatonin and cytokinin on alleviating drought-induced leaf senescence in creeping bentgrass (*Agrostis stolonifera*). *Environmental and Experimental Botany* 145:1–11
55. Bhattacharjee S. 2005. Reactive oxygen species and oxidative burst: roles in stress, senescence and signal transduction in plants. *Current Science* 89:1113–21
56. Ma X, Yu J, Zhuang L, Shi Y, Meyer W, et al. 2020. Differential regulatory pathways associated with drought-inhibition and post-drought recuperation of rhizome development in perennial grass. *Annals of Botany* 126:481–97
57. Sun S, Ma W, Mi C, Mao P. 2024. Telomerase reverse transcriptase, a telomere length maintenance protein in alfalfa (*Medicago sativa*), confers *Arabidopsis thaliana* seeds aging tolerance via modulation of telomere length. *International Journal of Biological Macromolecules* 277:134388

58. Ma D, Liu B, Ge L, Weng Y, Cao X, et al. 2021. Identification and characterization of regulatory pathways involved in early flowering in the new leaves of alfalfa (*Medicago sativa* L.) by transcriptome analysis. *BMC Plant Biology* 21:8
59. Chen C, Chen H, Zhang Y, Thomas HR, Frank MH, et al. 2020. TBtools: an integrative toolkit developed for interactive analyses of big biological data. *Molecular Plant* 13:1194−202
60. Geng G, Lv C, Stevanato P, Li R, Liu H, et al. 2019. Transcriptome analysis of salt-sensitive and tolerant genotypes reveals salt-tolerance metabolic pathways in sugar beet. *International Journal of Molecular Sciences* 20:5910
61. Dassanayake M, Larkin JC. 2017. Making plants break a sweat: the structure, function, and evolution of plant salt glands. *Frontiers in Plant Science* 8:406
62. Breckle SW. 1995. How do halophytes overcome salinity? In *Biology of Salt Tolerant Plants*. eds eds Khan MA,Ungar IA. Department of Botany, University of Karachi. pp. 199−213
63. Yamamoto A, Hashiguchi M, Akune R, Masumoto T, Muguerza M, et al. 2016. The relationship between salt gland density and sodium accumulation/secretion in a wide selection from three Zoysia species. *Australian Journal of Botany* 64:277−84
64. Semenova GA, Fomina IR, Biel KY. 2010. Structural features of the salt glands of the leaf of *Distichlis spicata* 'Yensen 4a' (Poaceae). *Protoplasma* 240:75−82
65. Oi T, Hirunagi K, Taniguchi M, Miyake H. 2013. Salt excretion from the salt glands in Rhodes grass (*Chloris gayana* Kunth) as evidenced by low-vacuum scanning electron microscopy. *Flora - Morphology, Distribution, Functional Ecology of Plants* 208:52−57
66. Li Q, Song J, Zhou Y, Chen Y, Zhang L, et al. 2022. Full-length transcriptomics reveals complex molecular mechanism of salt tolerance in *Bromus inermis* L. *Frontiers in Plant Science* 13:917338
67. Chinnusamy V, Jagendorf A, Zhu JK. 2005. Understanding and improving salt tolerance in plants. *Crop Science* 45:437−48
68. Bose J, Munns R, Shabala S, Gilliham M, Pogson B, et al. 2017. Chloroplast function and ion regulation in plants growing on saline soils: lessons from halophytes. *Journal of Experimental Botany* 68:3129−43
69. Zeng Z, Lin T, Zhao J, Zheng T, Xu L, et al. 2020. *OsHemA* gene, encoding glutamyl-tRNA reductase (GluTR) is essential for chlorophyll biosynthesis in rice (*Oryza sativa*). *Journal of Integrative Agriculture* 19:612−23
70. Gökçe AF, Gökçe ZNÖ, Junaid MD, Chaudhry UK. 2023. Evaluation of biochemical and molecular response of onion breeding lines to drought and salt stresses. *Scientia Horticulturae* 311:111802
71. Zhao S, Gao H, Luo J, Wang H, Dong Q, et al. 2020. Genome-wide analysis of the light-harvesting chlorophyll *a/b*-binding gene family in apple (*Malus domestica*) and functional characterization of *MdLhcb4.3*, which confers tolerance to drought and osmotic stress. *Plant Physiology and Biochemistry* 154:517−29
72. Møller IM. 2001. Plant mitochondria and oxidative stress: electron transport, NADPH turnover, and metabolism of reactive oxygen species. *Annual Review of Plant Biology* 52:561−91
73. Nagai S, Koide M, Takahashi S, Kikuta A, Aono M, et al. 2007. Induction of isoforms of tetrapyrrole biosynthetic enzymes, AtHEMA2 and AtFC1, under stress conditions and their physiological functions in Arabidopsis. *Plant Physiology* 144:1039−51
74. Beale SI. 2005. Green genes gleaned. *Trends in Plant Science* 10:309−12
75. Santos CV. 2004. Regulation of chlorophyll biosynthesis and degradation by salt stress in sunflower leaves. *Scientia Horticulturae* 103:93−99
76. Hotta Y, Tanaka T, Takaoka H, Takeuchi Y, Konnai M. 1997. New physiological effects of 5-aminolevulinic acid in plants: the increase of photosynthesis, chlorophyll content, and plant growth. *Bioscience, Biotechnology, and Biochemistry* 61:2025−28
77. Watanabe K, Tanaka T, Hotta Y, Kuramochi H, Takeuchi Y. 2000. Improving salt tolerance of cotton seedlings with 5-aminolevulinic acid. *Plant Growth Regulation* 32:99−103